Proceedings of the ASME 2016 International Mechanical Engineering Congress and Exposition
IMECE2016
November 11-17, 2016, Phoenix, Arizona, USA

IMECE2016-65729

THERMOELECTRIC EFFECTS OF SIZE OF MICROCHANNELS ON AN INTERNALLY COOLED LI-ION BATTERY CELL

Shahabeddin K. Mohammadian and Yuwen Zhang[1]
Department of Mechanical and Aerospace Engineering
University of Missouri
Columbia, MO, USA

ABSTRACT

Thermoelectric effects of size of microchannels on an internally cooled Li-ion battery cell is investigated in this paper. The liquid electrolyte was flowed as the coolant through rectangular microchannels embedded in the positive and negative electrodes. The effects of size of microchannels on the thermal and electrical performances of a Li-ion (Lithium-ion) battery cell were studied by carrying out *3D* transient thermal analysis. Six different cases were designed according to the ratio of the width of the microchannels to the width of the cell from *0* to *0.5*. The effects of inlet velocity of electrolyte flow, inlet temperature of electrolyte flow, and size of the microchannels were studied on the temperature uniformity inside the battery cell, maximum temperature inside the battery cell, and cell voltage. The results showed that increasing the size of the microchannels enhances the thermal performance of the battery cell; however, it causes slight decrease on the cell voltage (less than *2%*). Comparison between the case with width ratio of *0.5* (Case 6) with the case without microchannel (Case 1) showed that this internal cooling method can decrease the maximum temperature of the battery up to *11.22K*, *9.36K*, and *7.86K* for the inlet temperature of electrolyte flow of *288.15K*, *298.15K*, and *308.15K,* respectively. Furthermore, the case with width ratio of 0.5 (Case 6) has up to 77% better temperature uniformity compare with the case with width ratio of 0.1 (Case 2). Increasing the inlet temperature of electrolyte flow enhances the temperature uniformity up to 33% and increases the cell voltage up to 3%, but it keeps the battery on higher temperatures. Furthermore, increasing the inlet velocity of electrolyte flow from *0.01m/s* to *0.01m/s* enhances the thermal management of the battery cell by decreasing the temperature inside the battery up to *8.09K*, *6.75K*, and *5.67K* for the inlet temperature of electrolyte flow of *288.15K*, *298.15K*, and *308.15K* respectively. Furthermore, it improves the temperature uniformity up to *89%* and decreases the voltage less than *1%*.

INTRODUCTION

Sustainable and renewable energies like solar and wind are the best alternative sources of energy instead of fossil fuels. These sources of energy need to be stored. Li-ion batteries are one of the best candidates for storing and transporting them as electrical power. Li-ion batteries, same as other electrical storages generate heat during charge and discharge processes. This generated heat should be transferred out of the battery. Many researches were carried out for thermal management of these batteries. All the cooling methods that have been utilized to keep the Li-ion batteries in an appropriate thermal condition can be categorized as external or internal cooling methods.

Active external cooling methods, like air cooling and liquid cooling are the initial methods that attracted the attention of many researchers. Thermal behaviors of flat-plate and cylindrical batteries was investigated by Xun et al. [1]. They improved the cooling energy efficiency by increasing the cooling channel size. Mohammadian and Zhang [2] showed that higher temperature uniformity in addition to temperature reduction in an air cooled module using a special pin fin heat sink that the heights of pin fins increase linearly through the width of the air flow channel. On another study, He et al. [3] investigated an air cooled active control battery pack and showed that the combination of active controlling and air flow reciprocating can reduce the energy consumption required for cooling. Yang et al. [4] used liquid metals as coolant for a Li-ion battery pack. They found that under the same flow

[1] Corresponding author. Email: zhangyu@missouri.edu

conditions, lower temperature and higher temperature uniformity would be achieved using liquid metals compare with water.

Utilizing metal foams with air or liquid cooling methods is the second step of active cooling methods to improve the thermal management systems of Li-ion batteries. Mohammadian et al. [5] computationally studied an air-cooled Li-ion battery module which aluminum porous metal foam filled partially in the air flow duct. They showed that inserting aluminum metal foam in the airflow channel enhances the thermal performance of the Li-ion battery cell. Recently, Mohammadian and Zhang [6] utilized the combination of metal and non-metal foams for an air cooled Li-ion battery module. They found that partially use of ceramic foam as part of the heat sink combine with partially insert of aluminum foam in the air flow channel improves the temperature uniformity of the battery significantly.

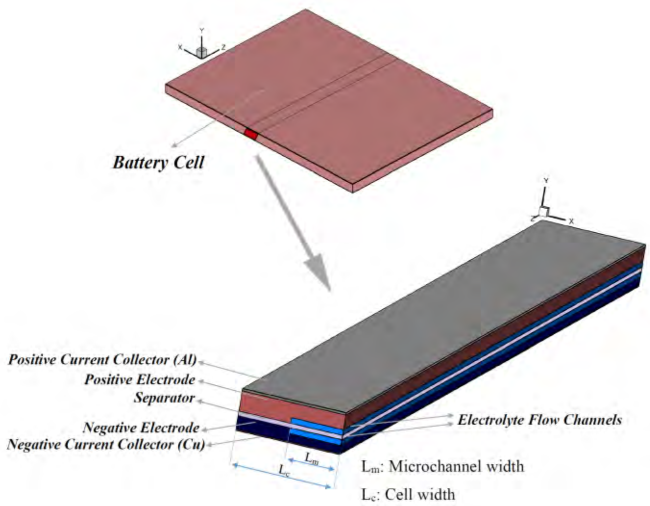

Fig. 1 Definition sketch

Passive external cooling methods have attracted the attention of some researchers. Javani et al. [7] computationally studied the effects of organic normal octadecane PCM on thermal management of a Li-ion battery cell. Their results showed 10% higher temperature uniformity applying *3mm* PCM and 3.04K lower temperature in the battery cell using *12mm* PCM compare with the case of without PCM. On another study, Wang et al. [8] added aluminum foam to the paraffin PCM. They found that the use of aluminum foam enhances the temperature uniformity of the PCM by speeding up the melting process and keeps the Li-ion battery in lower temperature. On a similar study, Samimi et al. [9] added carbon fibers to paraffin wax PCM to improve the temperature conductivity of the PCM. They showed that this new PCM composite can prepare a suitable medium for thermal management of a battery stack.

Due to the low thermal conductivity of Li-ion batteries, some researchers tried to cool them internally. An internally cooled system that utilized passive, liquid-vapor phase change processes was studied by Bandhauer and Garimella [10]. Mohammadian et al. [11] compared an internally cooled Li-ion battery module with an externally liquid cooled one and showed that internal cooling has higher thermal performance compare to external cooling. Although external cooling methods were studied by many researches, internal cooling ones are still new.

In this study, liquid electrolyte was flowed inside the microchannels that embedded in the positive and negative electrodes (Fig. 1). 3D transient thermal analysis of a Li-ion battery cell was done. Effects of size of microchannels on the Thermo-electrical performance of the battery cell were investigated as well as the effects of inlet temperature of electrolyte flow and velocity. Six different size of microchannels were designed and the effects of inlet temperature of electrolyte flow and velocity were studied on the maximum temperature of the cell, temperature uniformity inside the cell, and the cell voltage. The properties of the cell and the dimensions of the all six cases were tabulated in Table 1, and Table 2, respectively.

Table 1: Properties of the prismatic cell [11, 12]

	Thermal Conductivity ($Wm^{-1}K^{-1}$)	Density (kgm^{-3})	Specific Heat ($Jkg^{-1}K^{-1}$)	Viscosity ($kgm^{-1}s^{-1}$)
Electrolyte	*0.59*	*1223*	*1375*	*0.003*
Prismatic cell	*0.81 (Thickness direction)* *1.17 (along surfaces)*	*1965.2*	*1166*	-

Table 2: Dimensions of the different cases

	Microchannel Width (L_m) (mm)	Cell Width (L_c) (mm)	Microchannel thickness (μm)
Case 1	*0*	*1000*	*50*
Case 2	*100*	*1000*	*50*
Case 3	*200*	*1000*	*50*
Case 4	*300*	*1000*	*50*
Case 5	*400*	*1000*	*50*
Case 6	*500*	*1000*	*50*

NOMENCLATURE

a specific area of the battery (1/m)
a_p specific area of the positive electrode (1/m)
a_n specific area of the negative electrode (1/m)
DOD depth of discharge
E cell voltage (V)
E_{oc} open-circuit potential (V)
$\vec{i_p}$ linear current density vector in the positive electrode (A/m)
$\vec{i_n}$ linear current density vector in the negative electrode (A/m)
J current density (A/m^2)
Q_T theoretical capacity per unit area of the electrode (Ah/m^2)
q heat generation rate per unit volume (W/m^3)
r_p resistance of positive electrode (Ω)
r_n resistance of negative electrode (Ω)
SDT standard deviation of the temperature field inside the

	battery (K)
t	time duration (s)
V_p	potential of the positive electrode (V)
V_n	potential of the negative electrode (V)

MATHEMATICAL MODEL

In this study, just one symmetrical part of a *14.6 Ah* Li-ion battery cell ($LiMn_2O_4$ cathode, graphite anode) was considered. Figure 2 shows the geometry dimensions and boundary conditions. Following assumptions were considered to simplify the simulations:

- It was assumed that microchannels are not part of the battery cell and there is no electrochemical contact between the electrolyte flow and battery cell
- Electrodes and separator behave like solids instead of porous media. It was supposed that there is no electrolyte transport inside them.
- Inside the microchannels, just thermal behavior of the electrolyte flow was considered and electrochemical behaviors were neglected.
- Electrical current flows perpendicular to the electrode's surfaces
- Thermal radiation was negligible

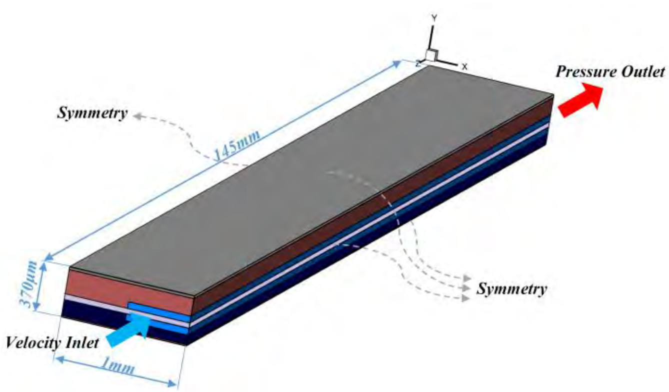

Fig. 2 Geometry dimensions and boundary conditions

Continuity of the electrical current on the electrodes leads to [13, 14]:

$$\nabla . i_p - J = 0 \quad (1)$$

$$\nabla . i_n + J = 0 \quad (2)$$

Where *J*, i_p, and i_n are current density, linear current density vector in positive electrode, and linear current density vector in negative electrode, respectively. Using Ohm's low for i_p and i_n:

$$\nabla^2 V_p = -r_p J \quad (3)$$

$$\nabla^2 V_n = -r_n J \quad (4)$$

where V_p , V_n, r_p, and r_n are the potential of the positive electrode, the potential of the negative electrode, the resistance of the positive electrode, and the resistance of the negative electrode, respectively.

The current density *J* can be defined as [13, 14]

$$J = Y\left(V_p - V_n - U\right) \quad (5)$$

where *Y* and *U* at *25°C* can be found as follow:

$$Y = 116.859 - 892.8001(DOD) + 5250.46(DOD)^2 - 13623.09(DOD)^3 + 1585317(DOD)^4 - 6757.8539(DOD)^5 \quad (6)$$

$$U = 4.12 - 0.804(DOD) + 1.075(DOD)^2 - 1.177(DOD)^3 \quad (7)$$

To modify *Y* and *U* for temperatures other than *25°C*, following correlations should be utilized [14]:

$$Y = Y_{25°C}\, exp\left\{-c_1\left(\frac{1}{T_{abs}} - \frac{1}{T_{abs,0}}\right)\right\} \quad (8)$$

$$U = U_{25°C} - c_2\left(T_{abs} - T_{abs,0}\right) \quad (9)$$

DOD can be calculated as follow:

$$DOD = \frac{\int_0^t J dt}{Q_T} \quad (10)$$

where *t* and Q_T are the charge time and the theoretical capacity per unit area of the electrodes.

The heat generation rate can be found as follow [14]:

$$q = aJ\left[E_{OC} - E - T\frac{dE_{OC}}{dT}\right] + a_p r_p i_p^2 + a_n r_n i_n^2 \quad (11)$$

where a, J, E_{OC}, E, a_p, and a_n are the specific area of the battery, the current density, the open-circuit potential of the cell, the cell voltage, the specific area of the positive electrode, and the specific area of the negative electrode, respectively.

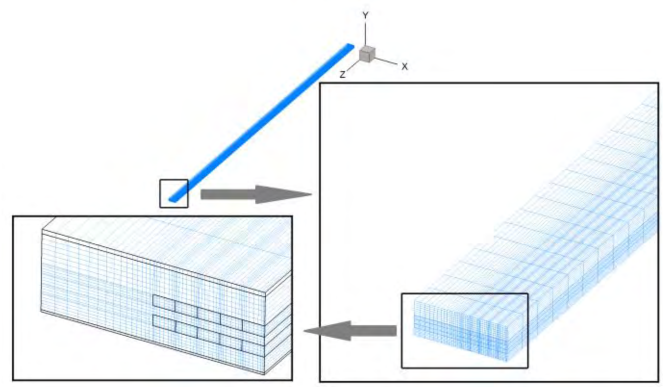

Fig. 3 Computational Grid

NUMERICAL SOLUTION

In this study, a pressure-based, transient model in Fluent was utilized. For integrating the governing equations, the time step was set to be *1s*. The convergence criterion was set 10^{-6} for flow and thermal energy.

Just one mesh was generated for all cases. As illustrated in Fig. 3, totally 13 volumes were generated. According to the number of each case, it was defined that how many volumes should be part of the microchannels. The other volumes were defined as part of the battery cell.

To study the grid sensitivity, this mesh adapted to times. First, second, and third grids consisted of 770,000, 1,155,000 and 1,535,380 cells, respectively. Table 3 illustrates the results of maximum temperature inside the battery cell and cell voltage after 600 seconds for case 1 at inlet temperature of 298.15 K. From this table, it can be found that the differences between the first and third grids are less than 0.02%. So, the first grid with 770,000 cells was utilized for main simulations in this study.

Table 3: Grid independency study (Case 1, 298.15 K, 600s)

# of Grids	*T_{Max} (K)*	*%*	*Cell Voltage (V)*	*%*
770,000	*307.76*		*3.40*	
1,155,000	*307.93*	*-0.04*	*3.42*	*0.54*
1,535,380	*307.81*	*0.02*	*3.40*	*0.01*

To validate the simulations, the results of Kim et al. [14] were chosen for comparison. The minimum temperatures of the battery cell extracted from Ref. [14] were considered for the discharge rate of *5C*; the same as discharge rate that have been used in this study. The results were obtained at the initial and environment temperature of *298.15 K*. Figure 4 shows this comparison. Good agreement is obvious between the results of this study and Kim et al. [14].

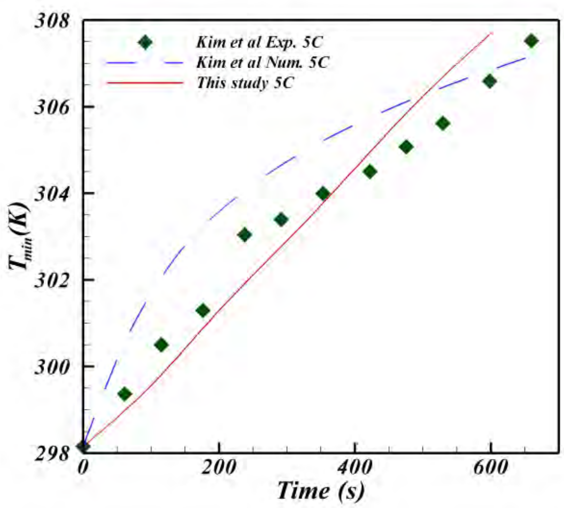

Fig. 4 Comparison of minimum temperature inside the battery

RESULTS AND DISCUSSIONS

The objective of this study was illustrating the effects of size of microchannels embedded in the electrodes on thermal and electrical performances of a Li-ion battery cell. The effects of inlet velocity of electrolyte flow, inlet temperature of electrolyte flow, and the size of microchannels were studied on the temperature reduction, temperature uniformity inside the battery pack, and cell voltage.

Figure 5 shows the variation of maximum temperature inside the battery cell for different inlet temperature of electrolyte flows. It is clear that, with increasing the size of the microchannels (Case 1 to Case 6), maximum temperature inside the battery decreases significantly. It happens due to the fact that increasing the size of the flow channel leads to higher heat transfer rate from the battery cell by increasing the heat transfer surface area.

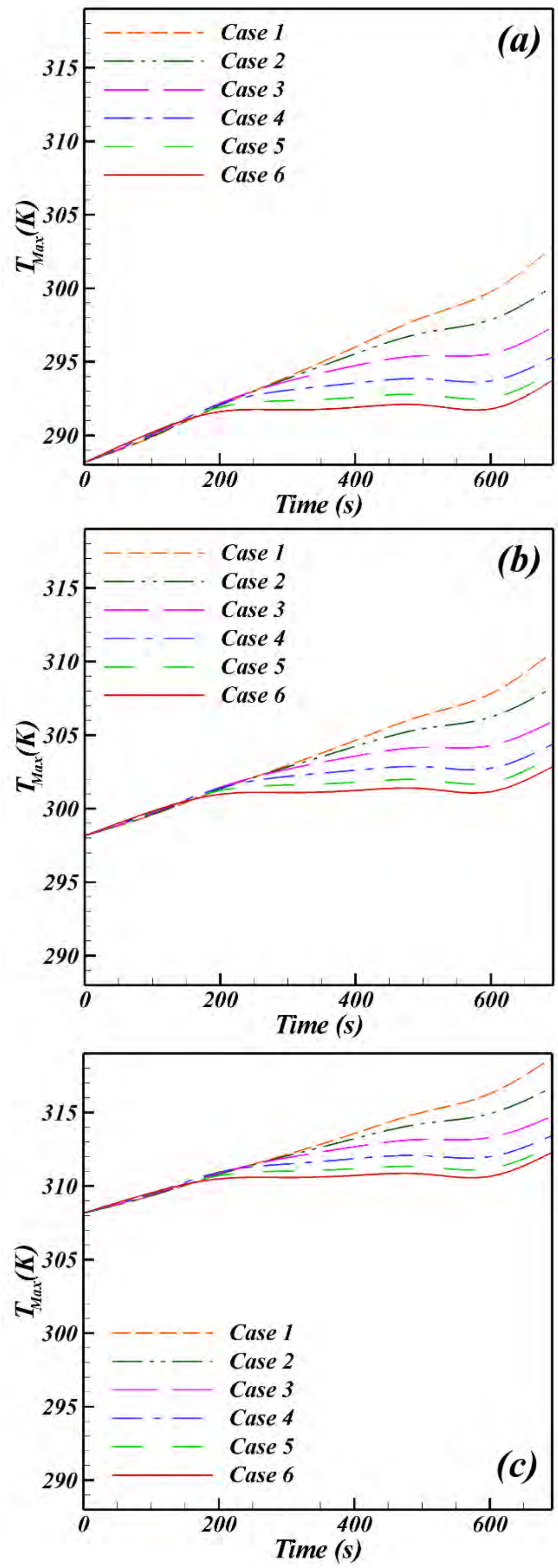

Fig. 5 Maximum temperature inside the battery cell versus time for inlet temperature of electrolyte flow of (a) 288.15K (b) 298.15K (c) 308.15K, and inlet velocity of electrolyte flow of 0.01 m/s.

Furthermore, increasing the size of the flow channels enhances the amount of the electrolyte mass flow rate (in a constant velocity) which again improves the heat transfer rate by increasing the temperature difference between the battery cell and electrolyte flow. Accordingly, the temperature inside the battery cell decreases. In comparison between the cases with microchannels with the case of without microchannels (Case 1), it was found that for inlet temperature of electrolyte flow of *308.15K* and after *600s*, maximum temperature inside the battery cell decreases up to *1.35K*, *2.97K*, *4.28K*, *5.09K*, and *5.62K* for Cases 2 to 6 respectively.

Also, it can be seen that, with increasing the inlet temperature of electrolyte flow, maximum temperature inside the battery increases for all cases which is due to the temperature difference reduction between the battery cell and electrolyte flow that decreases the heat transfer. Furthermore, this figure shows that differences between the maximum temperatures of the different cases decrease with increasing the inlet temperature of electrolyte flow. It is more clear for times between 600s and 690s. For instance, at the time of *600s*, the differences between the maximum temperatures of Case 1 and Case 6 are *7.94K*, *6.66K*, and *5.62K* respectively.

Figure 6 shows the variation of standard deviation of the temperature field (SDT) inside the battery cell versus time for different inlet temperature of electrolyte flows. It is obvious that, with increasing the inlet temperature of electrolyte flow, SDT inside the cell decreases for all cases. I.e., SDT decreases up to *33%* for all cases in comparison between the inlet temperature of electrolyte flow of *288.15K* and *308.15K*. Also, differences between the SDT for different cases decrease with increasing the inlet temperature of electrolyte flow. It is clearer for times between 600s to 690s.

Furthermore, it can be seen that with increasing the size of the microchannels (Case 3 to Case 6), SDT inside the cell decreases significantly that shows temperature uniformity improvement. It is because with increasing the size of the microchannels, the electrolyte mass flow rate and heat transfer surface area increase that leads to higher heat transfer from the battery cell. This higher heat transfer causes lower temperature inside the battery cell that leads to lower heat generation. Consequently, lower heat generation causes lower temperature that leads to temperature uniformity. The results showed up to *51%* SDT reduction when Case 6 compared with Case 2 for electrolyte inlet velocity of *0.01m/s* and at time step of *600*s.

Figure 7 shows the variation of the cell voltage versus time for different inlet temperature of electrolyte flows. It can be seen that, with increasing the inlet temperature of electrolyte flow, cell voltage increases for all cases. It is because the electrochemical performance of the battery cell is higher on higher temperatures. *2.4%* higher voltage was achieved by increasing the inlet temperature of electrolyte flow from *288.15K* to *308.15K*. Also, the differences between the cell voltages for different cases decreases with increasing the inlet temperature of electrolyte flow.

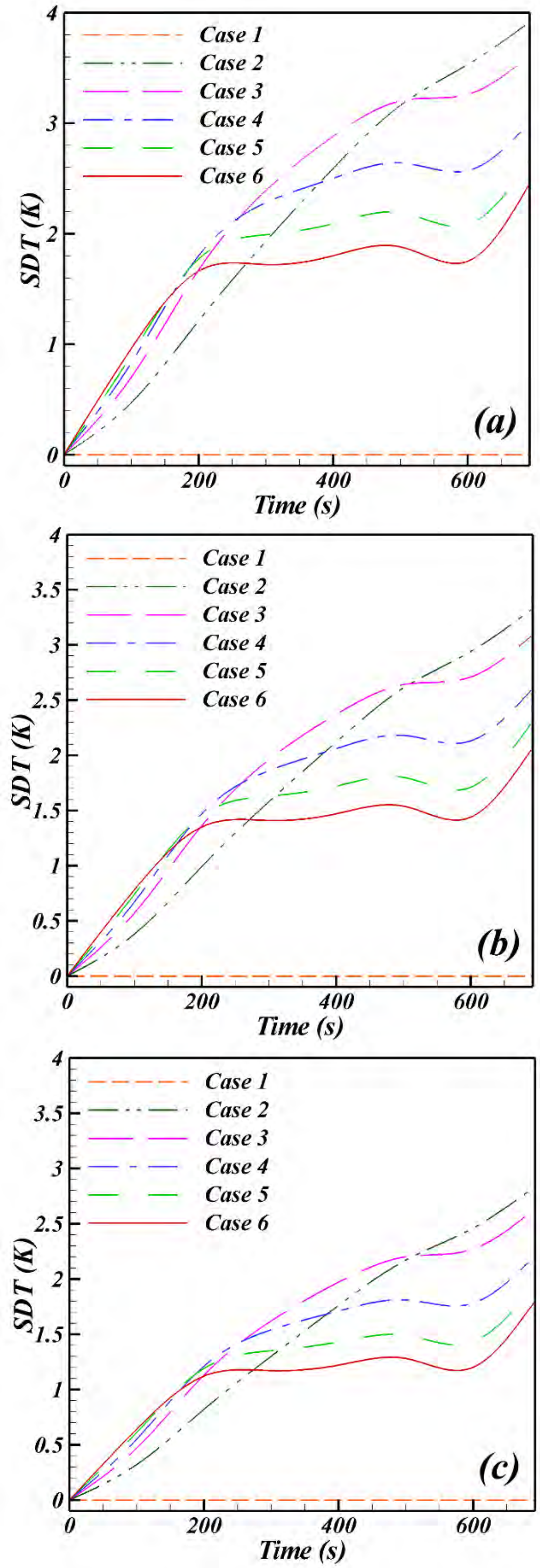

Fig. 6 SDT inside the battery cell versus time for inlet temperature of electrolyte flow of (a) 288.15K (b) 298.15K (c) 308.15K, and inlet velocity of electrolyte flow of 0.01 m/s.

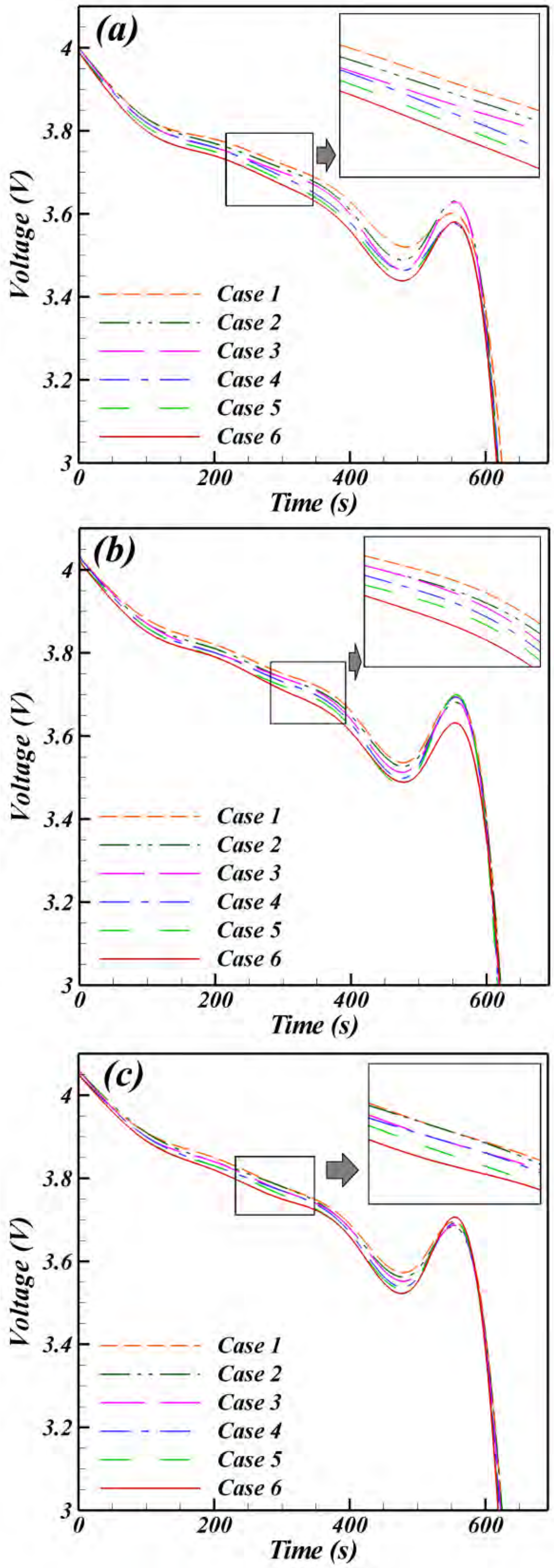

Fig. 7 cell voltage versus time for inlet temperature of electrolyte flow of (a) 288.15K (b) 298.15K (c) 308.15K, and inlet velocity of electrolyte flow of 0.01 m/s.

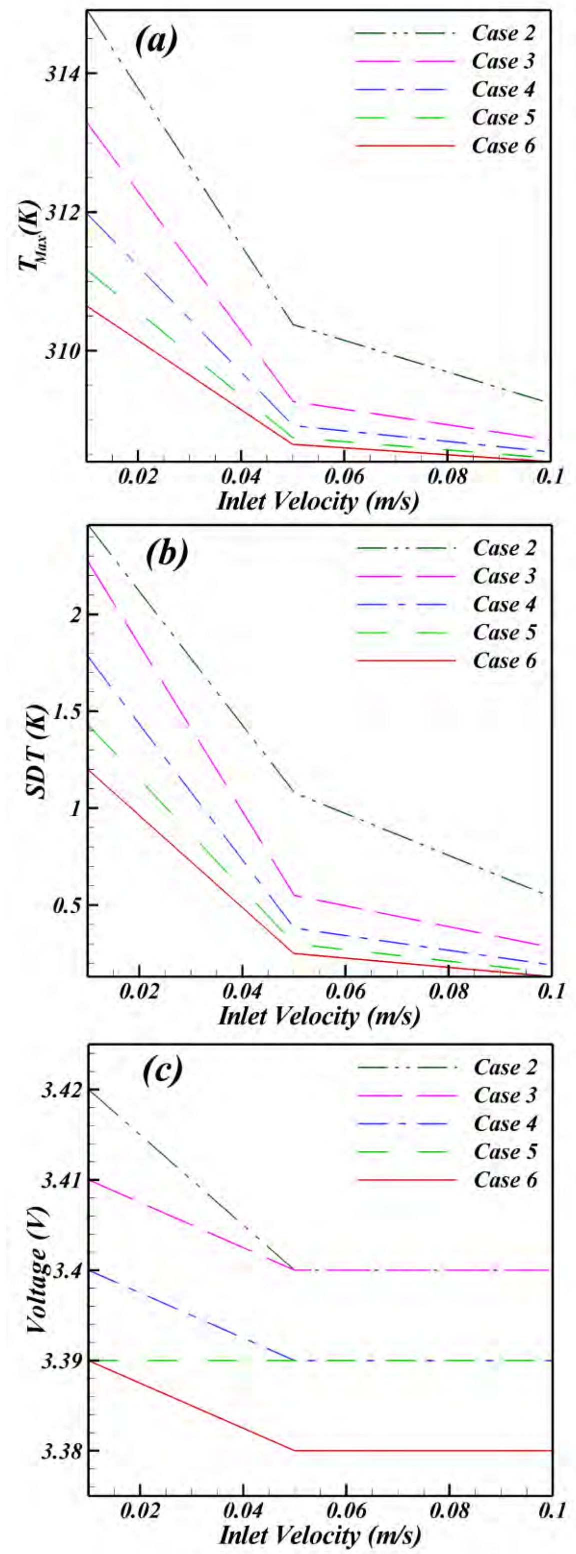

Fig. 8 (a) Maximum temperature (b) SDT inside the battery cell (c) cell voltage versus inlet velocity of electrolyte flow at the inlet temperature of electrolyte flow of 308.15K and 600s.

Furthermore, this figure shows that with increasing the size of the microchannels (Case 1 to Case 6), cell voltage decreases (up to *1.12%*). It is because with increasing the size of the microchannels, the effective volumes of the both positive and negative electrodes decrease that causes the cell voltage reduction.

Figure 8(a) shows the maximum temperature inside the battery cell versus inlet velocity of electrolyte flow at 308.15K and after 600s. It is clear that, with increasing the electrolyte flow velocity, maximum temperature inside the cell decreases. However, this reduction is less effective on higher flow velocities. It is because higher inlet flow velocities make lower temperature difference between the battery cell and cooling flow as the rate of heat generation is known. Here, it should be mentioned that, in thermal management of Li-ion batteries, the generated heat due to chemical reactions inside the battery cells should be transferred out of the battery. Since this heat generation reduces with temperature reduction, with increasing the electrolyte flow velocity more heat transfers from the battery cell that decreases the temperature inside the battery. Consequently, this temperature reduction decreases the rate of heat generation inside the battery cell. Increasing the inlet velocity of electrolyte flow from *0.01m/s* to *0.1m/s*, decreases the maximum temperature inside the battery cell up to *8.09K*, *6.75K*, and *5.67K* for inlet temperature of electrolyte flows of *288.15K*, *298.15K*, and *308.15K* respectively.

SDT for different cases has been illustrated in Fig. 8(b). It can be seen that, with increasing the inlet velocity SDT decreases. It is because higher inlet flow velocities transfer more heat from the battery cell that keeps the battery in lower temperatures. Consequently, it improves the temperature uniformity. Increasing the electrolyte inlet flow velocity from *0.01m/s* to *0.1m/s*, decreases the SDT up to *89%*.

Figure 8(c) shows the cell voltage for different cases versus inlet flow velocity. An interesting point of this figure is decreasing the cell voltage with increasing the inlet velocity of electrolyte flow till *0.05 m/s*. It is because electrochemical performance of Li-ion batteries is higher at higher temperatures. As mentioned earlier, increasing the inlet flow velocities leads to lower temperature field inside the battery cell that causes cell voltage reduction.

CONCLUSIONS

The effects of the size of microchannels, inlet temperature of electrolyte flow, and inlet velocity of electrolyte flow were investigated on the maximum temperature of the battery cell, SDT inside the battery cell, and cell voltage. The results showed that

- Enlarging the size of the microchannels, improves the thermal performance of the battery cell by decreasing the temperature inside the cell and enhancing the temperature uniformity. However, it leads to a small decrease of the cell voltage that is negligible (In the cases of this study).
- However, increasing the inlet temperature of electrolyte flow causes higher temperature field inside the battery, it improves the temperature uniformity and enhances the cell voltage.
- Increasing the inlet velocity of electrolyte flow decreases the temperature inside the battery and increases the temperature uniformity. Both of these effects enhances the thermal performance of the battery cell.
- According to the results, Case 6 is the best option in this study. As the purposes of the battery cooling are keeping the battery temperature in a safe temperature domain (not decreasing the temperature as low as possible), preparing higher temperature uniformity inside the battery cell, and having higher voltage finding optimum parameters requires more study by reducing the assumptions.

REFERENCES

[1] Xun, J., Liu, R., and Jiao, K., 2013, "Numerical and analytical modeling of lithium ion battery thermal behaviors with different cooling designs," Journal of Power Sources, 233, pp. 47-61.

[2] Mohammadian, S. K., and Zhang, Y., 2015, "Thermal management optimization of an air-cooled Li-ion battery module using pin-fin heat sinks for hybrid electric vehicles," Journal of Power Sources, 273, pp. 431-439.

[3] He, F., Wang, H., and Ma, L., 2015, "Experimental demonstration of active thermal control of a battery module consisting of multiple Li-ion cells," International Journal of Heat and Mass Transfer, 91, pp. 630-639.

[4] Yang, X.-H., Tan, S.-C., and Liu, J., 2016, "Thermal management of Li-ion battery with liquid metal," Energy Conversion and Management, 117, pp. 577-585.

[5] Mohammadian, S. K., Rassoulinejad-Mousavi, S. M., and Zhang, Y., 2015, "Thermal management improvement of an air-cooled high-power lithium-ion battery by embedding metal foam," Journal of Power Sources, 296, pp. 305-313.

[6] Mohammadian, S. K., and Zhang, Y., 2016, "Temperature Uniformity Improvement of an Air-Cooled High-Power Lithium-Ion Battery Using Metal and Nonmetal Foams," Journal of Heat Transfer, 138(11), pp. 114502-114502.

[7] Javani, N., Dincer, I., Naterer, G. F., and Yilbas, B. S., 2014, "Heat transfer and thermal management with PCMs in a Li-ion battery cell for electric vehicles," International Journal of Heat and Mass Transfer, 72, pp. 690-703.

[8] Wang, Z., Zhang, Z., Jia, L., and Yang, L., 2015, "Paraffin and paraffin/aluminum foam composite phase change material heat storage experimental study based on thermal management of Li-ion battery," Applied Thermal Engineering, 78, pp. 428-436.

[9] Samimi, F., Babapoor, A., Azizi, M., and Karimi, G., 2016, "Thermal management analysis of a Li-ion battery cell using phase change material loaded with carbon fibers," Energy, 96, pp. 355-371.

[10] Bandhauer, T. M., and Garimella, S., 2013, "Passive, internal thermal management system for batteries using microscale liquid–vapor phase change," Applied Thermal Engineering, 61(2), pp. 756-769.
[11] Mohammadian, S. K., He, Y.-L., and Zhang, Y., 2015, "Internal cooling of a lithium-ion battery using electrolyte as coolant through microchannels embedded inside the electrodes," Journal of Power Sources, 293, pp. 458-466.
[12] Cheng, L., Ke, C., Fengchun, S., Peng, T., and Hongwei, Z., 2009, "Research on Thermophysical Properties Identification and Thermal Analysis of EV Li-ion Battery," IEEE, pp. 1643-1648.
[13] Kwon, K. H., Shin, C. B., Kang, T. H., and Kim, C.-S., 2006, "A two-dimensional modeling of a lithium-polymer battery," Journal of Power Sources, 163(1), pp. 151-157.
[14] Kim, U. S., Yi, J., Shin, C. B., Han, T., and Park, S., 2011, "Modeling the Dependence of the Discharge Behavior of a Lithium-Ion Battery on the Environmental Temperature," J. Electrochem. Soc., 158(5), pp. A611-A618.